ACS OMEGA

http://pubs.acs.org/journal/acsodf

Article

Solubility of Piperine and Its Inclusion Complexes in Biorelevant Media and Their Effect on Attenuating Mouse Ileum Contractions

Toshinari Ezawa, Yukiko Inagaki, Kinami Kashiwaba, Namiko Matsumoto, Hajime Moteki, Isamu Murata, Yutaka Inoue,* Mitsutoshi Kimura, Masahiko Ogihara, and Ikuo Kanamoto

Cite This: *ACS Omega* 2021, 6, 6953−6964

Read Online

ACCESS | Metrics & More | Article Recommendations

ABSTRACT: This study evaluated the solubility of piperine (PP) in biorelevant media and the effect of its ground mixtures (GMs) and coprecipitates (CPs) on intestinal contractions when presented in inclusion complexes with α-, β-, and γ-cyclodextrins (CDs). In the powder X-ray diffraction (PXRD) and differential scanning calorimetry (DSC) measurements, CP (PP/αCD) and CP (PP/γCD) suggest the formation of inclusion complexes. The ^{1}H-nuclear magnetic resonance (NMR) analysis showed the integrated intensity ratios of CP (PP/αCD) and CP (PP/γCD) protons to be 1/2 and 1/1, the same as the respective molar ratios in the respective GM inclusion complexes. The intestinal contraction test confirmed that the intestinal contraction rate of carbachol (CCh) in the presence of 2.0×10^{-5} M PP was comparable to that in the absence of PP. On the other hand, CP (PP/αCD), GM (PP/αCD = 1/2), and GM (PP/βCD = 1/1) formed inclusion complexes that significantly suppressed the intestinal contractility at PP 1.0×10^{-8} M. No significant differences were observed between CP and GM. The solubility of the PP/αCD inclusion complex was 6−7 times higher than that of PP in the fasted-state-simulated intestinal fluid (FaSSIF, pH 6.5). PP functioned to suppress intestinal contraction by forming an inclusion complex. Based on this result, PP/αCD might be expected to be effective as an antidiarrheal.

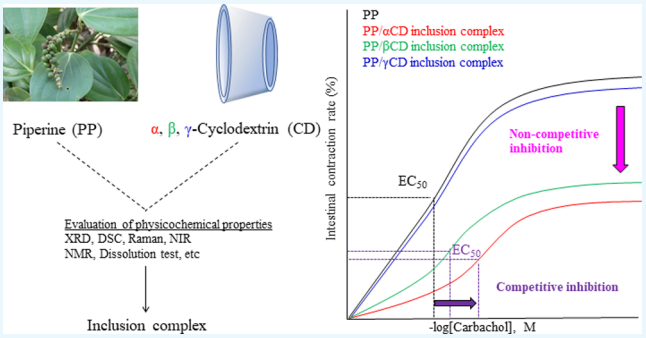

1. INTRODUCTION

Pepper is the most useful and important among all spices worldwide;[1] it has been used for home cooking, fever reduction, and as a carminative in Asian countries and Europe. The demand for pepper is expected to increase by 2% annually and the supply is expected to increase by 8−10%,[2] stimulated by the rapid development of seasonings and heightened health consciousness. Pepper is classified into black, white, green, etc., according to the processing method of Piperaceae (*Piper nigrum*). Black pepper contains 6−9% of piperine (PP), the pungent ingredient, compared to white pepper and green pepper.

PP [(2*E*,4*E*)-1-[5-(1,3-benzodioxol-5-yl)-1-oxo-2,4-pentadienyl]piperidine] is an amide with a methylenedioxyphenyl group, a pentadiene chain, and an amide substituent (piperidine). PP forms intramolecular conjugation from the amide group to the ether group of the methylenedioxyphenyl moiety. The steric position of the amide group of PP affects intramolecular conjugation; consequently, the change in the molecular energy affects its solubility.[3] PP has been reported to have antipyretic and intestinal contraction-regulating effects and is an important ingredient of pepper.[4] It has a muscarinic intestinal contractile effect, μ-opioid receptor activation, Ca^{2+} channel blocking effect, and other properties that affect the relaxation of intestinal contraction. It has been reported that the relaxation of intestinal contraction results from the inhibition of cAMP-mediated Cl^- secretion and suppression of Ca^{2+}-activated Cl^- channels.[5] Intestinal contraction and relaxation effects change the amount of wet feces excretion in mice depending on the dose of PP.[4] PP is considered to have a therapeutic effect on gastrointestinal motility disorders. PP is expected to be used as a laxative, an antidiarrheal, and a therapeutic agent for functional gastrointestinal disorders.

Cyclodextrins (CDs) are cyclic polysaccharides of D-glucopyranose linked by α-1,4 glycoside bonds. CDs are classified as α-, β-, and γ-CDs according to the number of D-glucopyranose units (6−8). The CD structure forms a central, hydrophobic cavity due to the ether groups located inside it, while the outer ring is hydrophilic. Brewster reported that CDs interact poorly with water-soluble drugs and drug candidates, resulting in an increase in their apparent water solubility.[6] Del Valle reported that CDs are useful molecular chelating agents;

Received: December 21, 2020
Accepted: February 18, 2021
Published: March 3, 2021

https://dx.doi.org/10.1021/acsomega.0c06198
ACS Omega 2021, 6, 6953−6964

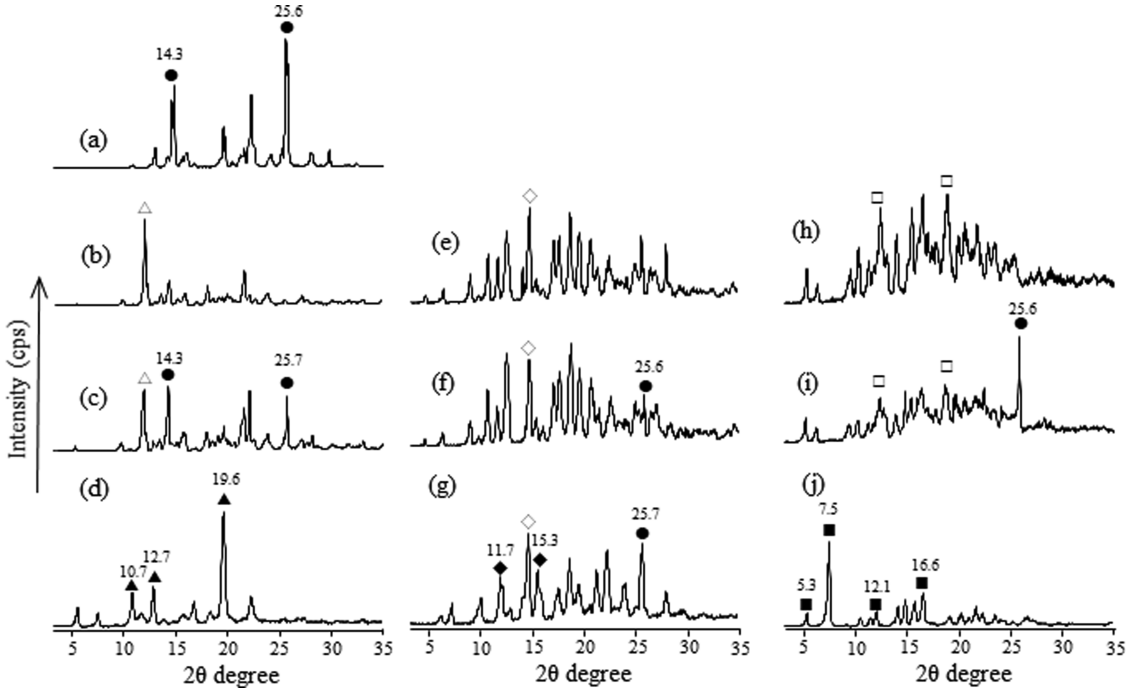

Figure 1. PXRD patterns of (a) PP intact, (b) αCD intact, (c) PM (PP/αCD = 1/2), (d) CP (PP/αCD), (e) βCD intact, (f) PM (PP/βCD = 1/1), (g) CP (PP/βCD), (h) γCD intact, (i) PM (PP/γCD = 1/1), and (j) CP (PP/γCD). ●: original PP, △: αCD original, ▲: channel, ◇: βCD original, ◆: head-to-head and head-to-tail, □: γCD original, ■: tetragonal.

owing to the supramolecular structures, they carry out chemical reactions that involve intramolecular interactions where covalent bonds are not formed between interacting molecules.[7] Tan reported that the taste of the bitterness component is masked by making the pyridostigmine bromide/βCD complex a dispersible tablet.[8] Also, the CD is used for controlled release of drugs,[9] protection of active ingredients against thermally accelerated decomposition,[10] and used to improve the antimicrobial activity,[11] solubility, and stability.[12] As an example, the results of phase-solubility studies showed that ellagic acid formed the inclusion complexes with βCD and (2-hydroxypropyl)-βCD in the molar ratio of 1:1 increased solubility, and the antioxidant activity of ellagic acid was increased.[13] Based on these findings, this study used nontoxic CDs, which are used as solubilizers for pharmaceuticals.[6]

Various methods such as ground mixtures (GMs) and coprecipitates (CPs) exist for the preparation of inclusion complexes. The GM method utilizes the mechanochemical effect to prepare an inclusion complex by a solid−solid reaction.[14] The preparation of inclusion complexes of PP with α-, β-, and γ-CDs using the GM method have already been reported.[15−17] The CP method uses an inclusion complex by a liquid−liquid reaction utilizing the difference in solubility between the drug and CD.[18] Physical mixtures (PMs) were prepared for comparison with GMs and CPs. The inclusion complex formation and solubility of caffeic acid/CD that differ depending on each CD and preparation method have been reported.[14,19]

Preparing the inclusion complex of PP with each CD by different methods may lead to an understanding of the chemical properties and inclusion complex formation that improves the poor water solubility of PP. Furthermore, from an inclusion complex formation, PP may increase the regulatory response of intestinal contractions. The biological activity of each inclusion complex may change to an action different from that of PP alone, depending on the CD used. The purpose of this study is to understand the physicochemical properties and guide the selection of specific PP/CD inclusion complexes for use in the regulation of intestinal contraction. Here, the PP/CD inclusion complexes were prepared using the coprecipitate method in addition to the previously reported GM method and used to evaluate the solubility in biorelevant media. Further, the effect on intestinal contractions by PP inclusion complexes with different CDs was evaluated.

2. RESULTS AND DISCUSSION

2.1. Powder X-ray Diffraction (PXRD) Measurements.

PXRD measurements were performed to examine the variation in the crystallinity of the PP/CD complexes (Figure 1). PP intact showed characteristic diffraction peaks (indicated by ●) at 2θ = 14.3 and 25.6°.

In the αCD system, PM (PP/αCD = 1/2) showed characteristic diffraction peaks of PP at 2θ = 14.3 and 25.7°. CP (PP/αCD) showed characteristic diffraction peaks of the inclusion complex due to channel-type crystals (indicated by ▲) at 2θ = 10.7, 12.7, and 19.6°.[20] This suggests that PP is bound in the αCD cavity and does not form the characteristic crystal sequence of PP.

In the βCD system, PM (PP/βCD = 1/1) showed a characteristic diffraction peak of PP at 2θ = 25.6°. GM (PP/βCD = 1/1) of the inclusion complex prepared by the ground mixture method lacked the characteristic crystal diffraction peak of PP.[15] On the other hand, CP (PP/βCD) showed characteristic diffraction peaks of head-to-head and head-to-tail (indicated by ◆) at 2θ = 11.7 and 15.3°, respectively, with PP-derived diffraction peaks seen at 2θ = 25.7°.[21,22]

In the γCD system, PM (PP/γCD = 1/1) showed a characteristic diffraction peak of PP at 2θ = 25.6°. CP (PP/γCD) showed characteristic tetragonal diffraction peaks (indicated by ■) at 2θ = 5.3, 7.5, 12.1, and 16.6°. The GM

https://dx.doi.org/10.1021/acsomega.0c06198
ACS Omega 2021, 6, 6953−6964

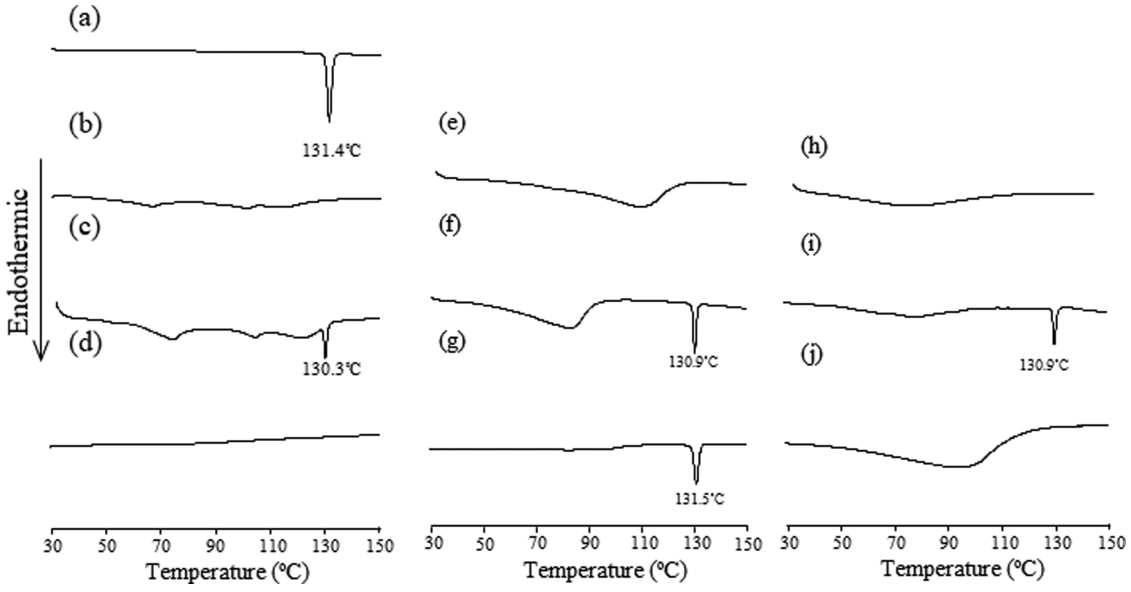

Figure 2. DSC curves of (a) PP intact, (b) αCD intact, (c) PM (PP/αCD = 1/2), (d) CP (PP/αCD), (e) βCD intact, (f) PM (PP/βCD = 1/1), (g) CP (PP/βCD), (h) γCD intact, (i) PM (PP/γCD = 1/1), and (j) CP (PP/γCD).

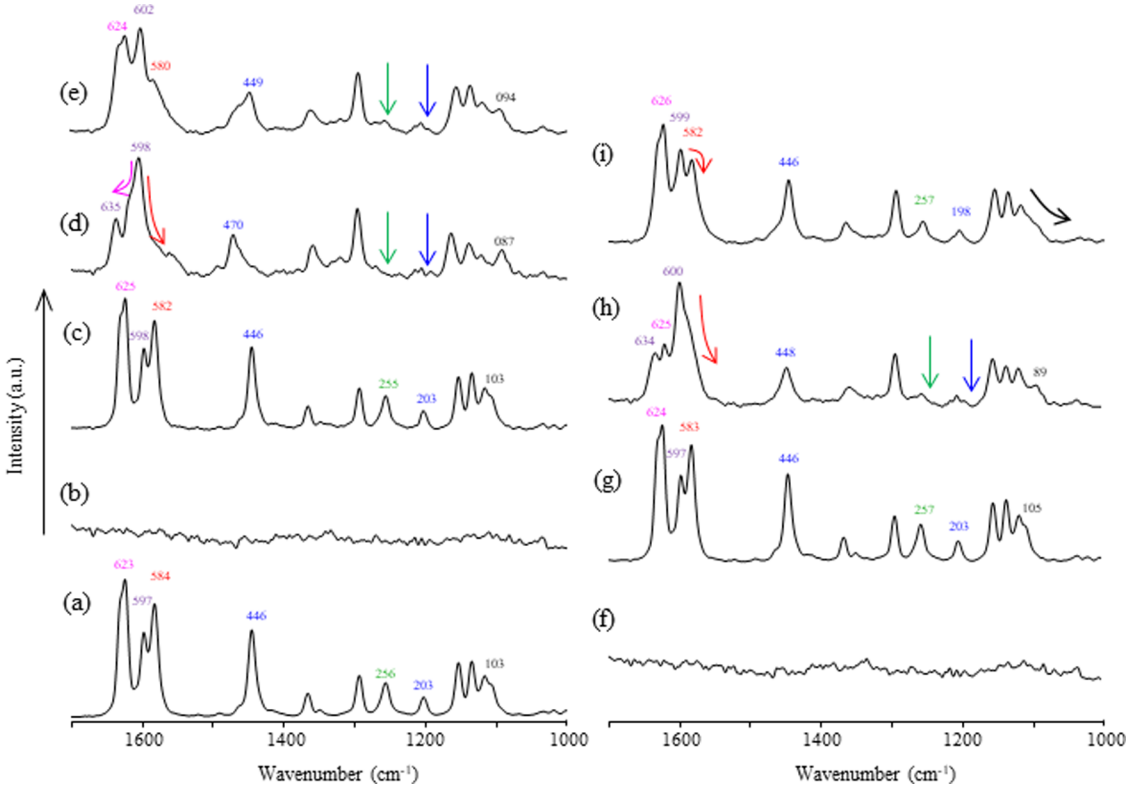

Figure 3. Raman spectra of (a) PP intact, (b) αCD intact, (c) PM (PP/αCD = 1/2), (d) CP (PP/αCD), (e) GM (PP/αCD = 1/2), (f) γCD intact, (g) PM (PP/γCD = 1/1), (h) CP (PP/γCD), and (i) GM (PP/γCD = 1/1).

(PP/γCD = 1/1) of the inclusion complex showed an amorphous crystal diffraction peak. When it was incubated at 40 °C and 82% RH for 1 week, multiple crystal diffraction peaks (tetragonal, monoclinic, and hexagonal) appeared.[17] The crystal structure of the CD inclusion complex changes depending on the water content and the inclusion form. It has been reported that the van der Waals forces and hydrogen bonds of inclusion complexes differ depending on the preparation method.[17] The appearance of multiple crystal diffraction peaks may result from the molecular motility of PP loosely associated with γCD. On the other hand, CP (PP/γCD) showed only the characteristic tetragonal diffraction peaks. It can be inferred from this that there was a difference between the coprecipitation and the GM method that contributed to the motility of PP molecules.

2.2. Differential Scanning Calorimetry (DSC) Measurements. DSC measurements were performed to confirm changes in the PP thermal behavior due to inclusion complex formation (Figure 2). The PP intact showed an endothermic peak at 131

https://dx.doi.org/10.1021/acsomega.0c06198
ACS Omega 2021, 6, 6953−6964

°C. PM (PP/αCD = 1/2), PM (PP/βCD = 1/1), and PM (PP/γCD = 1/1) showed an endothermic peak corresponding to the PP melting point at around 130 °C. In contrast, this peak was not seen for CP (PP/αCD) and CP (PP/γCD). The endothermic peak of the guest molecule disappeared upon the formation of the inclusion complex as previously reported by us for GM (PP/αCD = 1/2), GM (PP/βCD = 1/1), and GM (PP/γCD = 1/1).[15−17] Therefore, CP (PP/αCD) and CP (PP/γCD) formed an inclusion complex.[23] On the other hand, CP (PP/βCD) showed an endothermic peak corresponding to the PP melting point at approximately 131 °C. Since βCD forms strong hydrogen bonds at C_2− and C_3−OH of glucose, it has low solubility in water as compared with αCD and γCD.[24] The difference in the CD's solubility contributed to the formation of CP inclusion complexes and might have affected their thermal behavior.

2.3. Raman Spectroscopy. The results of PXRD and DSC measurements indicate the formation of inclusion complexes of PP with αCD and γCD (Figure 3). The PP structure contains single and double C−C bonds.

Raman spectroscopy easily detects different carbon−carbon bonds and has been used to evaluate differences in interactions between the GM and CP. The single-crystal X-ray analysis confirmed that the structure of PP does feature π−π stacking with the closest intermolecular contacts being carbon−carbon bonds.[15] NIR and solid-state fluorescence measurements revealed that the molecular behavior of PP inside the α, β, and γCD cavities changed by water and heat factors depends on the mobility of the methylenedioxyphenyl group.[16] Also, from a Raman spectroscopy measurement, PP/αCD, PP/βCD, and PP/γCD inclusion complexes prepared by the GM method have been confirmed to suppress the motility of the methylenedioxyphenyl group and pentadiene chain that are hydrophobic parts of PP.[17] From these reports, it is important to evaluate the carbon−carbon bonds of PP to understand the intermolecular interaction with CD.

The Raman spectrum of PP intact showed scattering bands for the aromatic C═C (1584 cm^{-1}), aliphatic C═C (1625 cm^{-1}), CH_2 (1203, 1448 cm^{-1}), O═C−N− (1597 cm^{-1}), ═C−O−C (1256 cm^{-1}), and CH (1103 cm^{-1}) (Figure 3a).

In the αCD systems, PM (PP/αCD = 1/2) indicated Raman scattering bands for the aromatic C═C (1582 cm^{-1}), aliphatic C═C (1625 cm^{-1}), CH_2 (1203, 1446 cm^{-1}), O═C−N− (1598 cm^{-1}), ═C−O−C (1255 cm^{-1}), and CH (1103 cm^{-1}) (Figure 3c). The GM (PP/αCD = 1/2) spectrum indicated broad scattering bands for the aromatic C═C and CH_2 groups, with reduced intensity. The scattering peak at 1104 cm^{-1} corresponding to the CH group of PP shifted to 1098 cm^{-1} (Figure 3e). The CP (PP/αCD) spectrum exhibited broad scattering bands for the aromatic C═C and pentadiene CH groups, with an amide group scattering peak at 1635 cm^{-1}. The scattering peak at 1103 cm^{-1} corresponding to the CH group of PP shifted to 1087 cm^{-1} (Figure 3d).

In the γCD systems, PM (PP/γCD = 1/1) indicated Raman scattering bands for the aromatic C═C (1583 cm^{-1}), aliphatic C═C (1624 cm^{-1}), CH_2 (1203, 1446 cm^{-1}), O═C−N− (1597 cm^{-1}), ═C−O−C (1257 cm^{-1}), and CH (1105 cm^{-1}) (Figure 3g). The GM (PP/γCD = 1/1) spectrum showed broad scattering bands for the CH peak and a reduced intensity of the aromatic C═C peak at 1582 cm^{-1} (Figure 3i). The CP (PP/γCD) spectrum showed broad scattering bands for the aromatic C═C, ═C−O−C, and CH_2 peaks, a reduced intensity of the pentadiene C═C peak at 1625 cm^{-1}, and the amide group scattering peak at 1634 cm^{-1} (Figure 3h). Depending on the CD's ring size, the αCD system significantly suppressed the motility of the aromatic ring and the pentadiene chain compared with the γCD system. PP is indicated to form an intramolecular bond from the amide group to the ether group of the methylenedioxyphenyl moiety. The coprecipitate method placed the aromatic ring and pentadiene chain of PP deeply inside the CD cavity compared to the GM method. The molecular motility of the amide group appeared to significantly distort the piperidine ring that is a nitrogen substituent.

2.4. ^{1}H-Nuclear Magnetic Resonance (NMR) Measurement. The molar ratio of CA with αCD and γCD in the CP was determined based on ^{1}H NMR spectroscopy (Figure 4). The

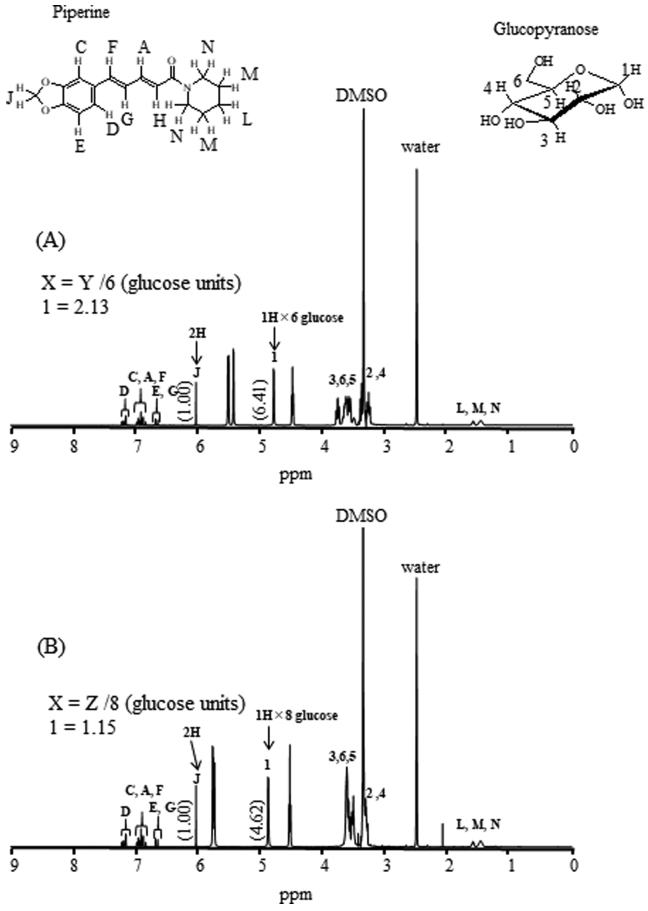

Figure 4. ^{1}H-NMR spectra of (A) CP (PP/αCD) and (B) CP (PP/γCD) in dimethyl sulfoxide (DMSO)-d_6.

ratios of the integrated intensity of H-J of PP and the integrated intensity of H-1 of αCD or γCD were calculated. The integrated intensity of H-1 of αCD was approximately 6.41 and that of H-J (2 protons) of PP was 1. The structure of αCD has 6 D-glucopyranose units linked together in a ring, so about 2 αCD molecules are present relative to each PP molecule. On the other hand, the integrated intensities of H-1 of αCD was about 4.62 and of H-J (2 protons) of PP was 1. γCD has 8 D-glucopyranose units linked together in a ring, so about 1 γCD molecule is present relative to each PP molecule. Therefore, CP (PP/αCD) and CP (PP/γCD) showed the same inclusion molar ratio of GM (PP/αCD = 1/2) and GM (PP/γCD = 1/1).

2.5. Examination of Dissolution Characteristics in the 1st Fluid for Dissolution Test. The solubility of PP and the

https://dx.doi.org/10.1021/acsomega.0c06198
ACS Omega 2021, 6, 6953−6964

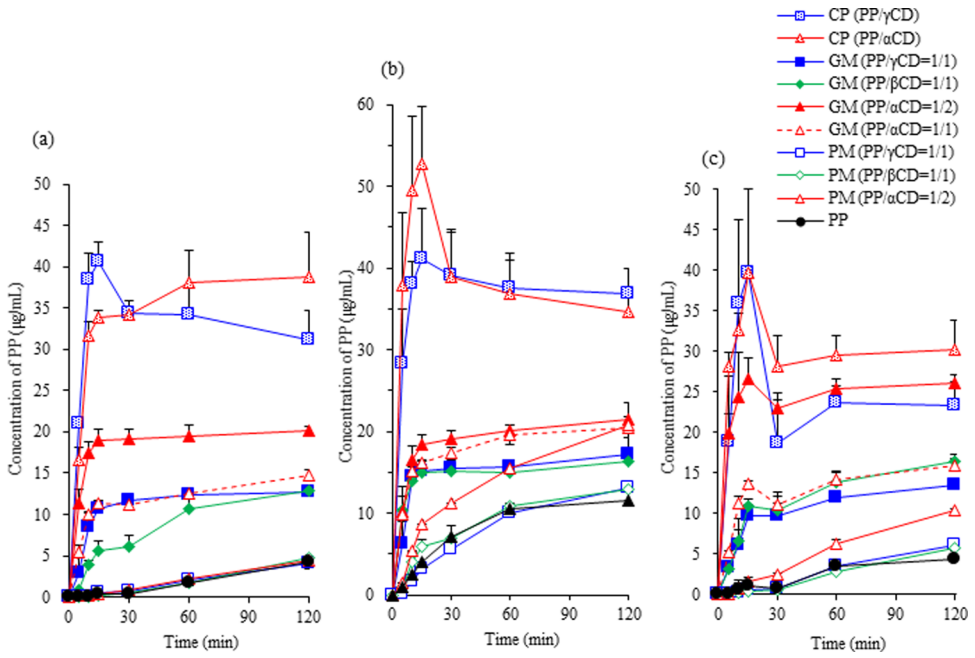

Figure 5. Dissolution profiles of PP with CDs in (a) first fluid for the dissolution test (pH 1.2, 900 mL), (b) FaSSIF (pH 6.5, 300 mL), and (c) FaSSIF (sodium taurocholate and lecithin not included, pH 6.5, 300 mL). Results were expressed as mean ± standard deviation (SD) (n = 3).

various inclusion complexes at pH 1.2 was evaluated (Figure 5a). The solubility of PP in the dissolution test (pH 1.2) first fluid was 4.2 μg/mL after 120 min. After 15 min of dissolution, GM (PP/αCD = 1/2) showed a high solubility of 19 μg/mL; no change in solubility was observed between 15 and 120 min. GM (PP/βCD = 1/1) showed a sustained-release dissolution behavior because it undergoes hydrophobic interactions compared to αCD and γCD. In coprecipitates, the high solubility of PP (PP/αCD) and CP (PP/γCD) was indicated compared with various GMs. CP (PP/γCD) showed a maximum solubility (40.5 μg/mL) in 15 min; supersaturation was induced by the salt and pH, and the solubility decreased to 31.1 μg/mL in 120 min. CP (PP/αCD) showed a maximum solubility (38.7 μg/mL) in 120 min without being affected by supersaturation. CP (PP/αCD) forms a stronger inclusion complex than GM and CP (PP/γCD). This suggests that the molecular arrangement and molecular morphology of PP in the CD cavity contribute to improved PP solubility.

2.6. Examination of Dissolution Characteristics in FaSSIF. A dissolution test was performed using FaSSIF to evaluate the intestinal solubility of PP and its inclusion complexes (Figure 5b).

The solubility of PP in FaSSIF was 11.6 μg/mL in 120 min; the solubility of GM (PP/αCD = 1/2) was 38.7 μg/mL in 120 min. The αCD systems of GM (PP/αCD = 1/1), GM (PP/αCD = 1/2), and PM (PP/αCD = 1/2) showed comparable solubility in 120 min. PP/αCD was confirmed to have higher solubility compared to PP/βCD and PP/γCD inclusion complexes prepared by the GM method. αCD has been reported to easily form inclusion complexes with phospholipids.[25] Also, the stability constant values of PP/αCD were reported to be $K_{\alpha 1/1}$ = 7473 M^{-1} and $K_{\alpha 1/2}$ = 47 M^{-1}.[16] Since the stability constant ($K_{\alpha 1/2}$) of PP/αCD = 1/2 showed a low value, the dissociated αCD forms an inclusion complex with lecithin. As a result, the proportion of PP/αCD = 1/1 inclusion complex increased leading to the higher solubility of PP. The solubility of PP was attributed to the molecular arrangement of PP that depended on the size of CD cycles. CP (PP/αCD) showed higher solubility (52.7 μg/mL) in 15 min compared to GM and CP (PP/γCD); its solubility decreased due to the supersaturation phenomenon but it showed a high value of 34.5 μg/mL in 120 min. The solubility of CP (PP/γCD) was 41.1 μg/mL in 15 min. It decreased to 36.8 μg/mL at 120 min due to the supersaturation phenomenon and showed the same solubility as CP (PP/αCD). The reason for the high solubilities of CP (PP/αCD) and CP (PP/γCD) might be that, based on Raman spectra data, the CPs significantly suppressed the aromatic ring and pentadiene chain of PP molecules compared to GMs. A strong inclusion complex was formed (Figure 3). Taurocholic acid and lecithin are major components of gallbladder bile that solubilize fat-soluble substances; both have been reported to form mixed micelles and increase the absorption of cholesterol from the small intestinal lumen.[26] The solubilization behavior of the CP inclusion complex showed high solubility aided by taurocholic acid and lecithin. In the absence of taurocholic acid and lecithin, the solubilities of CP (PP/αCD) and CP (PP/γCD) were the same at 15 min. At 120 min, CP (PP/γCD) showed lower solubility compared to CP (PP/αCD), affected by the supersaturation phenomenon (Figure 5c). In the presence of taurocholic acid and lecithin, CP (PP/γCD) was less affected by the supersaturation phenomenon than CP (PP/αCD), possibly because αCD has been reported to easily form the inclusion complex with lecithin. Furthermore, guest drugs of the γCD inclusion complex can be easily encapsulated in taurocholic acid.[27] With CP (PP/αCD), the solubilized PP molecules were incorporated into the mixed micelles with αCD forming an inclusion complex with lecithin that induced the supersaturation phenomenon. With CP (PP/γCD), PP was encapsulated in taurocholic acid that helped to maintain solubility.

2.7. Evaluation of Fluorescence in the Liquid State. Depending on the molecular orientation of molecules, the fluorescence wavelength is known to differ for the excited and ground states.[28] The increase in the fluorescence intensity due to CD indicates the formation of inclusion complexes; hydro-

https://dx.doi.org/10.1021/acsomega.0c06198
ACS Omega 2021, 6, 6953−6964

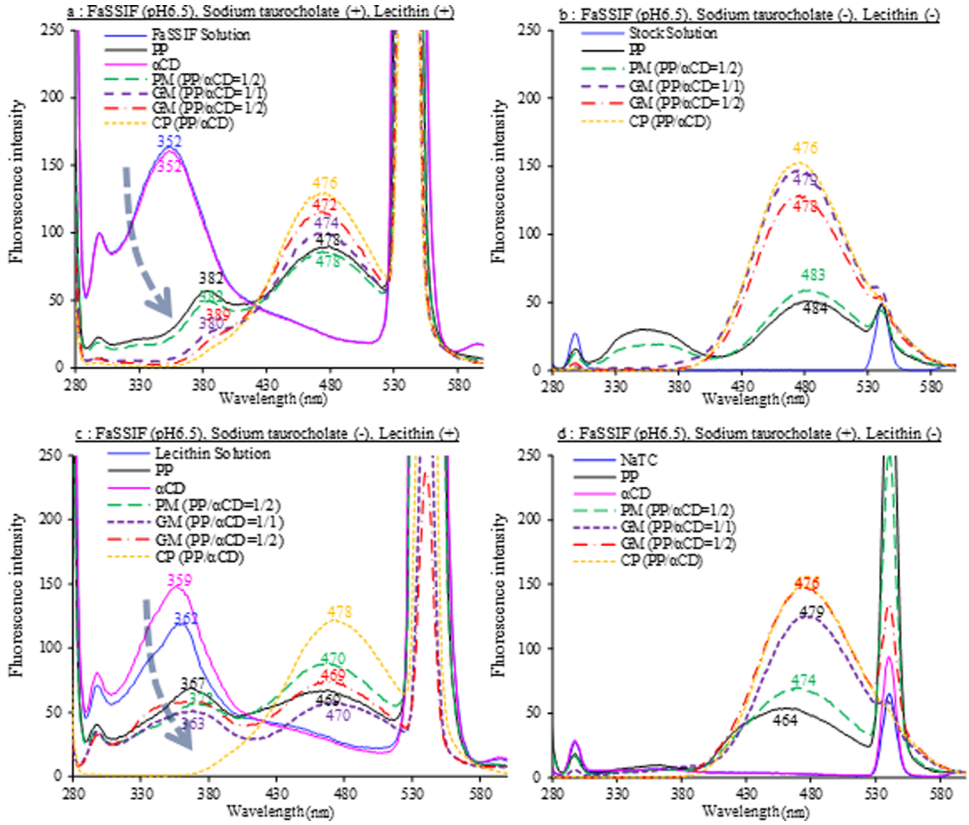

Figure 6. Changes in the emission spectra of the PP/αCD complex system (λ_{ex} = 270 nm). (a) FaSSIF, (b) FaSSIF (sodium taurocholate and lecithin not included), (c) FaSSIF (sodium taurocholate not included), and (d) FaSSIF (lecithin not included).

phobic interactions decrease the fluorescence maximum wavelength of PP.[29,30] Thus, the fluorescence spectrum measurements were performed to evaluate the molecular behavior that might contribute to the PP's solubility in FaSSIF. In the FaSSIF solution, Raman scattered light was detected at 399 nm, and the secondary scattered light due to excitation light was at 540 nm (Figures 6 and 7− 8a−d). The maximum fluorescence wavelength of the lecithin solution was seen at 362 nm (Figures 6 and 7−8 c). The maximum fluorescence wavelength of lecithin was blue-shifted (362−359 nm) when each CD was added to the lecithin solution (6Figures 6 and 7−88c). This suggests that the shift to the lower wavelength was due to the hydrophobic interactions between lecithin and the inside of the CD cavity.

In the FaSSIF solution in the presence of taurocholic acid and lecithin, the maximum fluorescence wavelength was seen at 352 nm. This suggested a mixed micelle formation (Figures 8 and 9−10a). PP intact, PM (PP/αCD = 1/2), PM (PP/βCD = 1/1), and PM (PP/γCD = 1/1) were confirmed at 382, 478, 378, and 380 nm (Figures 6 and 7−8a), respectively. Debnath and Mishra reported that PP exhibited higher-order micelle aggregates at the maximum fluorescence wavelength near 380 nm in the presence of taurocholic acid.[31] Thus, PP intact and PM (PP/αCD = 1/2) appear to form higher-order micelle aggregates in the FaSSIF solution. GM (PP/αCD = 1/1) and GM (PP/αCD = 1/2) showed a decreased fluorescence intensity at approximately 380 nm and an increased fluorescence maximum wavelength intensity at approximately 470 nm compared with PP and PM (PP/αCD-1/2) (Figure 6a). CP (PP/αCD) did not easily form higher-order micelle aggregates compared with GMs. In GM (PP/βCD = 1/1), the fluorescence intensity around 380 nm decreased and the fluorescence intensity around 470 nm was equivalent to that of PP intact (Figure 7a). These results suggest that GM (PP/βCD = 1/1) was solubilized in the FaSSIF solution without forming higher-order micelle aggregates. The maximum fluorescence wavelength of GM (PP/γCD = 1/1) was at 369 nm (Figure 8a). In the lecithin solution, PP showed the maximum fluorescence wavelength at 367 nm likely due to the formation of higher-order micelle aggregates (Figures 6 and 7−8c). Therefore, the fluorescence maximum wavelength of GM (PP/γCD = 1/1) in the FaSSIF solution indicates a higher-order micelle aggregate formation. The fluorescence intensity of CP (PP/γCD) decreased significantly around 380 nm and the maximum fluorescence wavelength was observed at approximately 480 nm (Figure 10a), suggesting that the solubility difference between CPs and GMs was influenced not only by the formation of strong PP/CD inclusion complexes but also by higher-order micelle aggregate formation.

2.8. Evaluation of the Intestinal Contraction Effect. Molecular mobility and solubility of PP were confirmed to be different depending on the CDs and preparation method. From a pharmacological point of view, this study focused on the intestinal contraction-regulating effect, which is the main function of PP, and evaluated the difference in the effect due to inclusion complex formation (Figures 9 and 10−11).

The Magnus method was performed using carbachol (CCh).[5] CCh is a synthetic choline ester drug that exhibits muscarinic and nicotine-like effects. These effects induce intestinal contraction by increasing spontaneous excitement. Since PP has been reported to have a muscarinic intestinal contractile effect, the contractile response of the intestine was induced with CCh and the effects of PP/CD inclusion complexes on the contractile response were examined.

https://dx.doi.org/10.1021/acsomega.0c06198
ACS Omega 2021, 6, 6953−6964

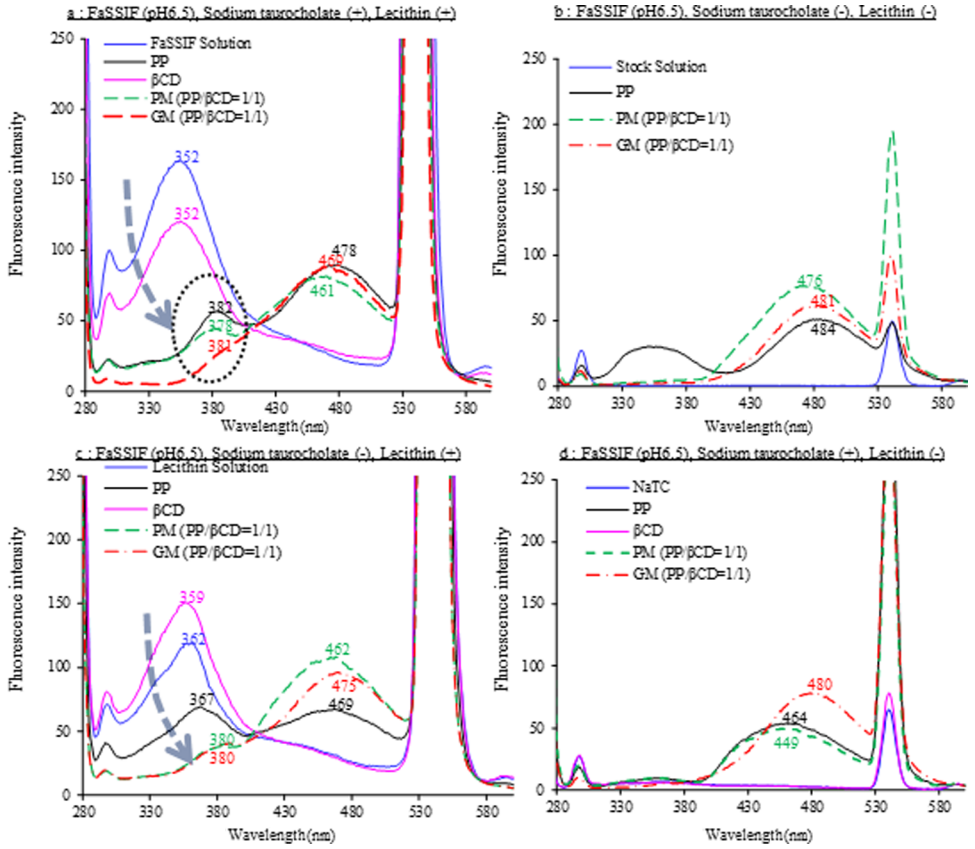

Figure 7. Changes in the emission spectra of the PP/βCD complex system (λ_{ex} = 270 nm). (a) FaSSIF, (b) FaSSIF (sodium taurocholate and lecithin not included), (c) FaSSIF (sodium taurocholate not included), and (d) FaSSIF (lecithin not included).

The ileal contraction rate of CCh was evaluated in the presence of various PP concentrations (Figure 11). With CCh, the intestinal tract began to contract at 1.0×10^{-10} M, with a maximum response at 1.0×10^{-7} M. The maximum contraction response induced by CCh was not significantly different from that exerted by 1.0×10^{-6} to 6.67×10^{-6} M PP but an increase in shrinkage by 120−140% was observed. This suggests that the muscarinic effect of PP may contribute to intestinal contraction. PP at 2.0×10^{-5} M exhibited almost the same behavior as the contractile response of CCh.

Based on the above data, PP alone, PMs, GMs, and CPs were used at 2.0×10^{-5} M PP.

In αCD systems, the contractions of αCD induced with 1.0×10^{-8} M CCh were approximately 114% of the largest contractile response. PP alone and PM (PP/αCD = 1/2) showed no significant difference in the ileum contraction response to CCh. Contractions of GM (PP/αCD = 1/1) induced with 1.0×10^{-8} M CCh were approximately 58% of the largest contractile response. GM (PP/αCD = 1/1) was not significantly different from PP alone but a tendency to suppress the ileum contraction response was noted. Contractions of GM (PP/αCD = 1/2) and CP (PP/αCD) induced with 1.0×10^{-7} M CCh were about 49.2 and 38.5%, respectively, of the largest contractile response, compared with PP alone, showing a significant statistical significance. Furthermore, the CCh concentration eliciting 50% of the largest contractile response (EC_{50}) of GM (PP/αCD = 1/2) and CP (PP/αCD) was higher compared with PP alone. No significant difference was found between GM (PP/αCD = 1/2) and CP (PP/αCD) (Figure 10a).

Contractions of βCD induced with 1.0×10^{-8} M CCh were approximately 115% of the largest contractile response but were not significantly different from PP alone and PM (PP/βCD = 1/1). GM (PP/βCD = 1/1) suppressed the largest contractile response by 30.5 and 31.6% compared with PP alone and PM, respectively. The EC_{50} of PP was between 1.0×10^{-10} and 1.0×10^{-9} M CCh. The EC_{50} of GM (PP/βCD = 1/1) changed to between 1.0×10^{-9} and 1.0×10^{-8} M CCh (Figure 10b).

Contractions of γCD induced with 1.0×10^{-7} M CCh were approximately 82% of the largest contractile response and not significantly different from PP alone and PM (PP/γCD = 1/1). Contractions of GM (PP/γCD = 1/1) and CP (PP/γCD) induced with 1.0×10^{-7} M CCh were about 50 and 51% of the largest contractile response, respectively, and not significantly different from PP alone. No significant difference was found between GM (PP/γCD = 1/1) and CP (PP/γCD) (Figure 10c). The fact that the PP/γCD inclusion complex has a low stability constant, forms weak hydrogen bonds, and exerts low intermolecular forces may explain why its inclusion complex showed no significant difference from PP alone.

At 1.0×10^{-7} M CCh, GM (PP/αCD = 1/2), CP (PP/αCD), and GM (PP/βCD = 1/1) significantly suppressed the contractile response compared with PP (Figure 12c). Since an increase in EC_{50} was confirmed for these three inclusion complexes, competitive inhibition of the muscarinic M_3 receptor was suggested (Figure 12a,b). According to previous studies, the stability constant values of PP/αCD were found to be $K_{1/1}$ = 7473 and $K_{1/2}$ = 47 M^{-1} and those for PP/βCD and PP/γCD $K_{1/1}$ = 3244 and 248 M^{-1}, respectively. The above result suggests that αCD is more likely to form an inclusion complex with PP

https://dx.doi.org/10.1021/acsomega.0c06198
ACS Omega 2021, 6, 6953−6964

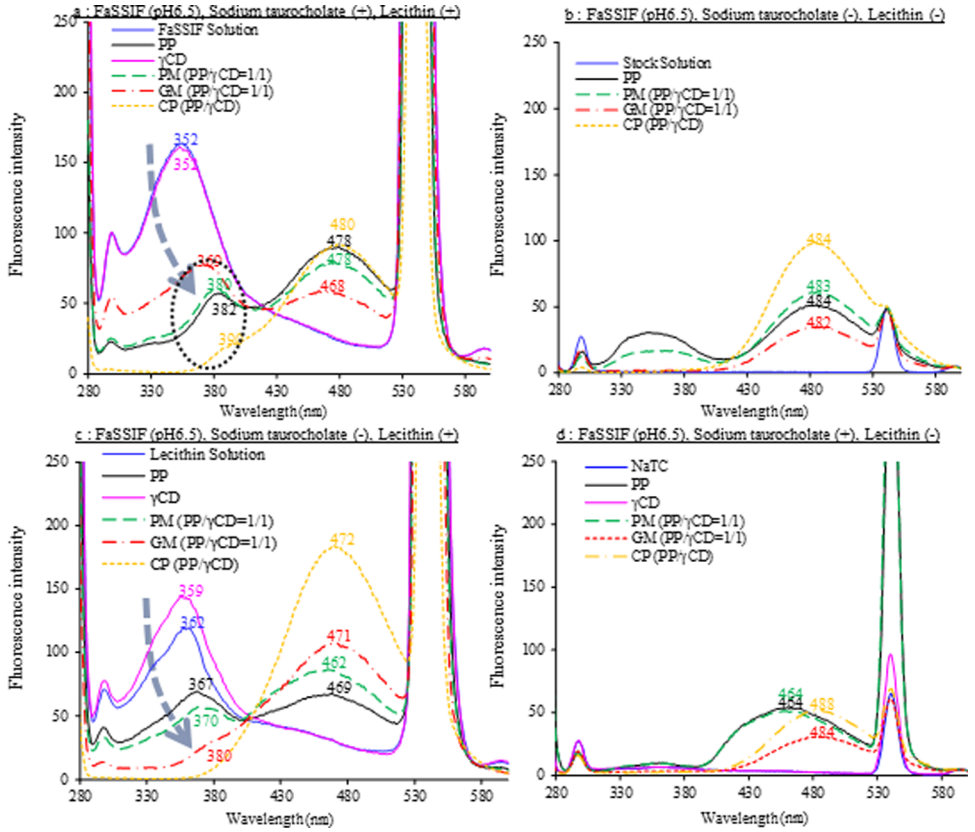

Figure 8. Changes in the emission spectra of the PP/γCD complex system (λ_{ex} = 270 nm). (a) FaSSIF, (b) FaSSIF (sodium taurocholate and lecithin not included), (c) FaSSIF (sodium taurocholate not included), and (d) FaSSIF (lecithin not included).

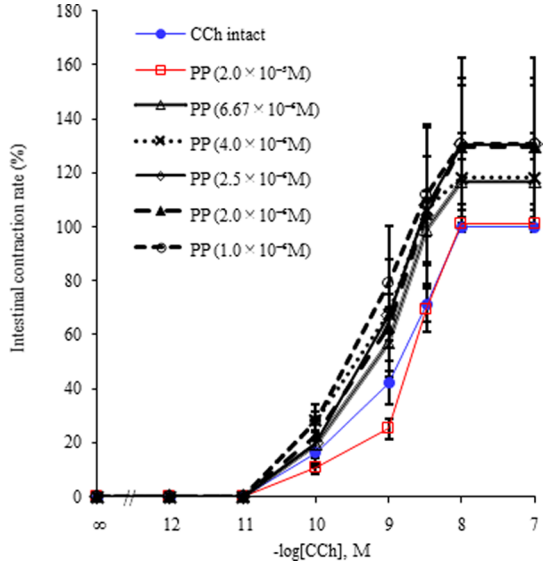

Figure 9. Concentration vs response curves of CCh in the absence and the presence of increasing concentrations of piperine, evaluated by the one-way analysis of variance followed by Dunnett's test. *p < 0.05 vs CCh.

than β- and γ-CDs.[17] Raman spectra measurements also suggested that the PP/αCD inclusion complex significantly suppressed the molecular motility of PP (Figure 3). PMs do not significantly suppress the intestinal contractile response compared to GMs and CPs. The solid-state formation of inclusion complexes appears to contribute to pharmacological effects. Since the largest contractile response is suppressed compared to PP, the effect of inclusion complexes may involve some noncompetitive inhibition. In other words, the inclusion complexes may act not only on the muscarinic M_3 receptor but also other specific intestinal contraction inhibitory effects that may be different from those of PP. In silico studies, Haque reported that the aromatic ring of PP shows a hydrogen bond with tryptophan 503 present in the protein pocket of the muscarinic acetylcholine receptor.[32] Also, PP has piperidine and amide as well as loperamide. di Bosco reported that loperamide exhibits a hydrogen bond between the protonated nitrogen of the piperidine ring and the carboxylic acid group of asparagine in the protein pocket of the opioid μ receptor.[33] That is, depending on the inclusion complex style, PP exposed from the inclusion complex may have shown different effects than PP alone. Although the detailed mechanism of the action is unknown, the inclusion complexes inhibit muscarinic M_3 receptor-mediated competition. Also, cAMP-induced protein kinase A activation and IP_3-induced Ca^{2+} emission control are expected. In the safety assessment by the FAO/WHO Joint Expert Committee on Food Additives, the acceptable daily intake was defined as "up to 5 mg/kg/day" for βCD. Moreover, γCD is rapidly and completely digested by pancreatic amylase. Among various PP/CD inclusion complexes, GM (PP/αCD = 1/2) and CP (PP/αCD) may have potential use as antidiarrheals and therapeutic agents for functional gastrointestinal disorders.

3. CONCLUSIONS

The intestinal contraction test confirmed that PP/αCD and GM PP/βCD inclusion complexes suppressed the contractile response of the ileum via competitive and noncompetitive inhibitions. PP/CD inclusion complexes have a unique

https://dx.doi.org/10.1021/acsomega.0c06198
ACS Omega 2021, 6, 6953−6964

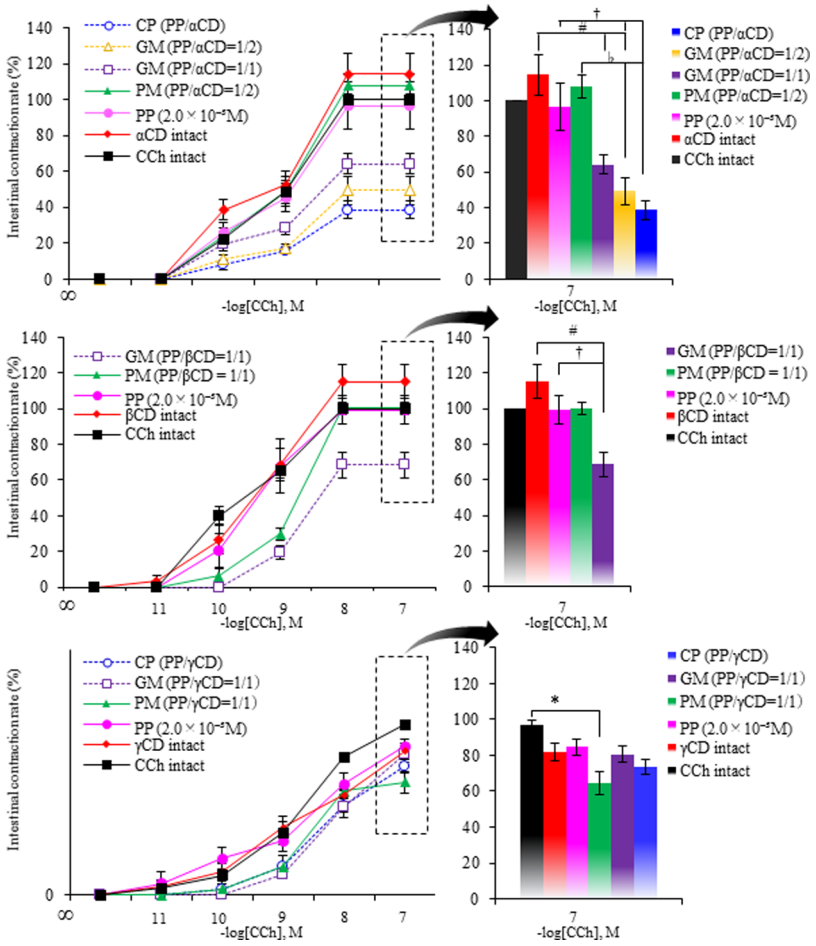

Figure 10. Change in the contractile response of the ileum by PP/CD inclusion complexes. Values are shown as mean ± standard error of the mean (SEM), (n = 5). Examined by the one-way analysis of variance followed by Tukey's test. *p < 0.05 vs CCh, #p < 0.05 vs CD, †p < 0.05 vs PP, and μp < 0.05 vs PM.

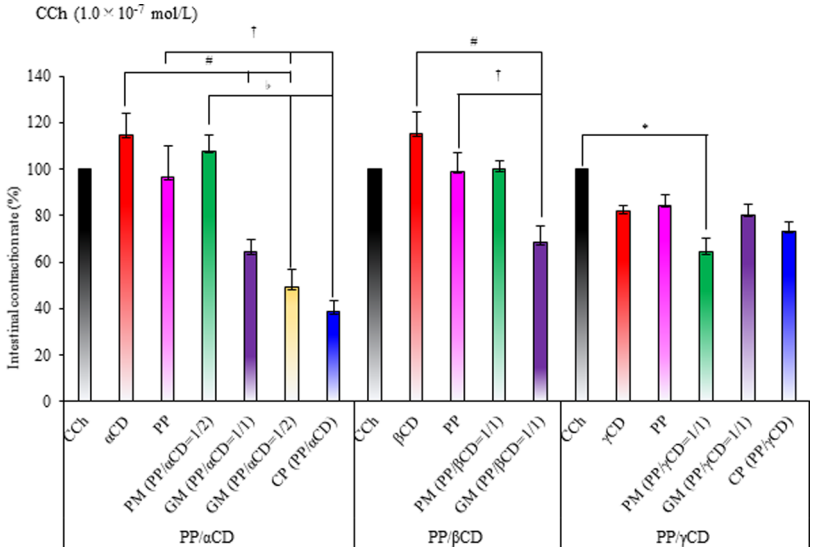

Figure 11. Change in the contractile response of the ileum by PP/CD inclusion complexes. Values are shown as mean ± SEM, (n = 5). Concentration of CCh is 1.0×10^{-7} mol/L. Evaluated by the one-way analysis of variance followed by Tukey's test. *p < 0.05 vs Cch, #p < 0.05 vs CD, †p < 0.05 vs PP, and μp < 0.05 vs PM.

pharmacological function that is different from PP alone. No significant difference was found between the GMs and CPs. In the FaSSIF dissolution test, CP (PP/αCD) and CP (PP/γCD) showed a higher solubility compared to GMs. The solubility of the inclusion complexes was higher than the PP concentration of 2.0×10^{-5} M (5.7 μg/mL) that suppressed the intestinal

https://dx.doi.org/10.1021/acsomega.0c06198
ACS Omega 2021, 6, 6953−6964

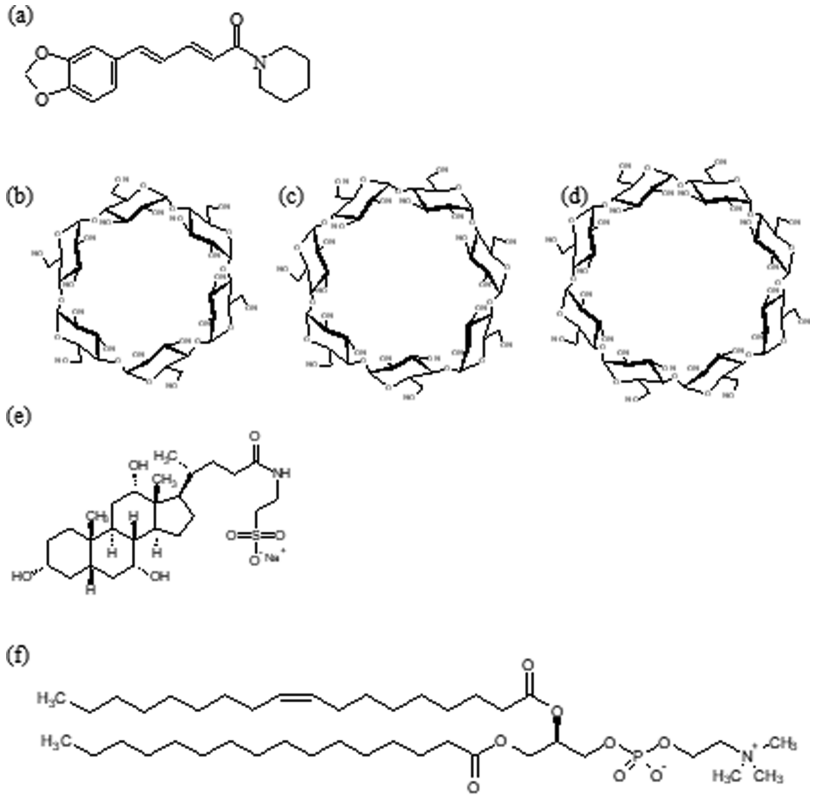

Figure 12. Chemical structures of (a) PP, (b) αCD, (c) βCD, (d) γCD, (e) NaTC, and (f) lecithin.

contractile response. Therefore, GM (PP/αCD = 1/2) and CP (PP/αCD) are expected to be used as antidiarrheals and therapeutic agents for functional gastrointestinal disorders.

4. MATERIALS AND METHODS

4.1. Materials. *4.1.1. Chemicals.* PP was purchased from FUJIFILM Wako Pure Chemical Co., Ltd. αCD, βCD, and γCD were donated by Cyclo Chem Co., Ltd. (Tokyo, Japan) and stored at 40 °C and 82% RH for 7 days. The humidity was controlled to obtain αCD 6.6-hydrate, βCD 10.5-hydrate, and γCD 12-hydrate (Figure 12). All other chemicals were purchased from Wako Pure Chemical Co., Ltd.

4.1.2. Preparation of the Inclusion Complex. It was reported that the GM method molar generated inclusion complexes having ratios PP/αCD = 1/2, PP/βCD = 1/1, and PP/γCD = 1/1.[15−17] PP/CD inclusion complexes were prepared with optimal inclusion molar ratios. GM was prepared by grinding the samples (1.0 g) for 60 min using a vibration rod mill (TI-500ET, CMT Co.) at a molar ratio of PP/αCD 6.6-hydrate = 1/2 and PP/βCD 10.5-hydrate = 1/1.

A coprecipitate (CP) was prepared by dropwise addition of 5 mL of an acetone solution of PP (0.11 mmol/mL) to 5 mL of an aqueous solution of CDs (0.11 mmol/mL). The solution was stirred for 1 h at 60 °C and then allowed to stand at room temperature for 24 h. The sample was filtered through a filter paper, and the precipitate was washed with 5 mL of acetone and vacuum-dried in a desiccator for 24 h.

4.2. Methods. *4.2.1. PXRD Measurements.* Changes in the samples' crystal diffraction patterns were measured using a powder X-ray diffractometer (MiniFlex II, Rigaku). The irradiation dose was a Cu wire. The diffraction intensity was measured using a NaI scintillation counter. Measurements were carried out at a voltage of 30 kV, current of 15 mA, a scan range of 2θ = 3−35°, and a scan rate of 4°/min.

4.2.2. DSC Measurements. The thermal behavior of the PP, CDs, and CP was determined using a differential scanning calorimeter (Thermo plus Evo, Rigaku) with a N_2 gas flow rate of 60 mL/min and a heating rate of 5 °C/min. Samples weighing approximately 3 mg were placed in an aluminum pan.

4.2.3. Raman Spectroscopy Measurements. Raman spectra of samples were recorded on a Cart-Mountable Raman Rxn2TM Analyzer-1000 nm, KAISER spectrometer with a scan range of 1000−1700 cm^{-1}, a spectral resolution of 5 cm^{-1}, an f/1.8 imaging spectrometer with a holographic transmission grating and a detector (TE-Cooled, 1024 Array Detector).

4.2.4. Fluorescence Spectrum Measurements of the Liquid State in FaSSIF. Fluorescence spectra of the liquid state were measured using a fluorescence spectroscopic altimeter (RF-5300pc, Shimadzu) at an excitation wavelength of 270 nm, an excitation and fluorescence bandwidth of 5 nm, and a measurement range of 280−600 nm.

4.2.5. ^{1}H-Nuclear Magnetic Resonance (NMR) Spectra Determination. The ^{1}H NMR spectra (1D) of the samples in DMSO were measured using an NMR spectrometer (Varian NMR System 400, Agilent) at a pulse width of 90°, relaxation delay of 6.4 μs, the scan time of 3.723 s, and a temperature of 295 K. The molar ratio of PP to αCD or γCD was calculated using eqs 1 and 2

$$X = Y/6 \quad (1)$$

$$X = Z/8 \quad (2)$$

where X is the number of CD molecules per 1 PP molecule, Y is the integrated intensity of H-1 in αCD, and Z is the integrated intensity of H-1 in γCD.

https://dx.doi.org/10.1021/acsomega.0c06198
ACS Omega 2021, 6, 6953−6964

Table 1. Composition of Dissolution Media

ingredient	first liquid of the pharmacopoeia	Tyrode's	FaSSIF (sodium taurocholate and lecithin are not included)	FaSSIF
pH	1.2	6.5	6.5	6.5
HCl	7 mL/L			
NaOH			∼13.80 mM	∼13.80 mM
NaCl	2 g/L	134 mM	134 mM	134 mM
KCl		2.68 mM		
$NaHCO_3$		11.9 mM		
NaH_2PO_4			∼28.66 mM	∼28.66 mM
$NaH_2PO_4{\cdot}2H_2O$		0.417 mM		
$MgCl{\cdot}6H_2O$		1.05 mM		
$CaCl_2{\cdot}2H_2O$		1.8 mM		
glucose		5.56 mM		
sodium taurocholate				3 mM
lecithin				0.75 mM

4.2.6. Dissolution Test. Dissolution testing was carried out according to the paddle method described in the 17th edition of the Japanese Pharmacopoeia, using the first fluid for dissolution test (pH 1.2, 900 mL) and FaSSIF (pH 6.5, 300 mL) as test media. The amount of the FaSSIF test solution was set to 300 mL to mimic the water content of the human gastrointestinal tract. FaSSIF's composition mimics the upper small intestine gastrointestinal environment (Table 1). It was prepared by including taurocholic acid and lecithin from the stock solution.

4.2.7. Preparation of the Ileum. Male ddY mice were fasted for 24 h and sacrificed by severing the cervical vertebrae. The abdominal wall was opened, and the small intestine was removed. The ileum specimens of the small intestine approximately 1.5 cm long were prepared. The animal experiments were conducted according to the Josai University guidelines and were approved by the University's Committee on Laboratory Animal Care.

4.2.8. Isolated Ileum (Magnus Technique). The isolated ileum was suspended in 50 mL of Tyrode's solution. Oxygen was supplied to a bath at 34−36 °C at a rate of 3−5 bubbles (radius: 0.5 mm) per second. Preparations (PP, CD, PM, GM, and CP) were subjected to a dissolution test involving Tyrode's solution and the resulting solutions served as test solutions.

4.2.9. Determination of the Ileum Contraction Height. Specimens of the ileum with verified contractility were washed twice with 50 mL of Tyrode's solution and immersed in 50 mL of fresh Tyrode's solution in an organ bath. The isolated ileum was left for approximately 3 min to adjust to the bath temperature. Test solution (100 μL) was added and allowed to elute PP for about 3 min as the ileum adjusted. Carbachol (CCh) was added cumulatively to induce ileal contractions. The intestinal contraction rate after the addition of each test article was calculated as a ratio with the maximum contraction height (100%) of 10^{-7} M CCh.

4.2.10. Statistical Analysis. A one-way analysis of variance was performed to compare the means of the study samples. After that, all groups were compared using Tukey's test to determine the significance of differences between the test groups. The *P*-values < 0.05 were considered statistically significant. All sample measurements were performed at $n = 5$.

AUTHOR INFORMATION

Corresponding Author

Yutaka Inoue − *Laboratory of Drug Safety Management, Faculty of Pharmacy and Pharmaceutical Sciences, Josai University, Sakado, Saitama 3500295, Japan;* orcid.org/0000-0003-3419-343X; Phone: +81-49-271-7980; Email: yinoue@josai.ac.jp

Authors

Toshinari Ezawa − *Laboratory of Drug Safety Management, Faculty of Pharmacy and Pharmaceutical Sciences, Josai University, Sakado, Saitama 3500295, Japan*

Yukiko Inagaki − *Laboratory of Clinical Pharmacology, Faculty of Pharmacy and Pharmaceutical Sciences, Josai University, Sakado, Saitama 3500295, Japan*

Kinami Kashiwaba − *Laboratory of Clinical Pharmacology, Faculty of Pharmacy and Pharmaceutical Sciences, Josai University, Sakado, Saitama 3500295, Japan*

Namiko Matsumoto − *Laboratory of Clinical Pharmacology, Faculty of Pharmacy and Pharmaceutical Sciences, Josai University, Sakado, Saitama 3500295, Japan*

Hajime Moteki − *Laboratory of Clinical Pharmacology, Faculty of Pharmacy and Pharmaceutical Sciences, Josai University, Sakado, Saitama 3500295, Japan*

Isamu Murata − *Laboratory of Drug Safety Management, Faculty of Pharmacy and Pharmaceutical Sciences, Josai University, Sakado, Saitama 3500295, Japan*

Mitsutoshi Kimura − *Laboratory of Clinical Pharmacology, Faculty of Pharmacy and Pharmaceutical Sciences, Josai University, Sakado, Saitama 3500295, Japan*

Masahiko Ogihara − *Laboratory of Clinical Pharmacology, Faculty of Pharmacy and Pharmaceutical Sciences, Josai University, Sakado, Saitama 3500295, Japan*

Ikuo Kanamoto − *Laboratory of Drug Safety Management, Faculty of Pharmacy and Pharmaceutical Sciences, Josai University, Sakado, Saitama 3500295, Japan*

Complete contact information is available at: https://pubs.acs.org/10.1021/acsomega.0c06198

Funding

This research was supported by Josai University.

Notes

The authors declare no competing financial interest.

ACKNOWLEDGMENTS

The authors wish to thank Cyclo Chem Co., Ltd. for providing α-, β-, and γ-CDs and the Department of Physical Chemistry, Hoshi University, for providing support for Raman spectroscopy. The TOC graphic photo was provided by Professor Yoshiaki Shirataki, Ph.D., at the Faculty of Pharmacy and Pharmaceutical Sciences, Josai University.

https://dx.doi.org/10.1021/acsomega.0c06198
ACS Omega 2021, 6, 6953−6964

■ ABBREVIATIONS USED

PP, piperine; CD, cyclodextrin; GM, ground mixture; CP, coprecipitate; PM, physical mixture; CCh, carbachol; PXRD, powder X-ray diffraction; FaSSIF, fasted-state simulated intestinal fluid; DSC, differential scanning calorimetry; C_2−OH, hydroxyl group attached to the carbon at position 2 of glucose; C_3−OH, hydroxyl group attached to the carbon at position 3 of glucose

■ REFERENCES

(1) Ravindran, P. N.; Kallupurakal, J. A. Black Pepper. In *Handbook of Herbs and Spices*, 2nd ed.; Peter, K. V., Ed.; Woodhead Publishing, Ltd, 2012; pp 86−115.

(2) Vietnam pepper association not hopeful of global price recopery; Vietnam+. https://en.vietnamplus.vn/vietnam-pepper-association-not-hopeful-of-global-price-recovery/152500.vnp.

(3) Pfund, L. Y.; Chamberlin, B. L.; Matzger, A. J. The bioenhancer piperine is at least trimorphic. *Cryst. Growth Des.* **2015**, *15*, 2047−2051.

(4) Mehmood, M. H.; Gilani, A. H. Pharmacological basis for the medicinal use of black pepper and piperine in gastrointestinal disorders. *J. Med. Food.* **2010**, *13*, 1086−1096.

(5) Pongkorpsakol, P.; Wongkrasant, P.; Kumpun, S.; Chatsudthipong, V.; Muanprasat, C. Inhibition of intestinal chloride secretion by piperine as a cellular basis for the anti-secretory effect of black peppers. *Pharmacol. Res.* **2015**, *100*, 271−280.

(6) Brewster, M. E.; Loftsson, T. Cyclodextrins as pharmaceutical solubilizers. *Adv. Drug Delivery Rev.* **2007**, *59*, 645−666.

(7) Del Valle, E. M. M. Cyclodextrins and their uses: a review. *Process Biochem.* **2004**, *39*, 1033−1046.

(8) Tan, Q.; Zhang, L.; Zhang, L.; Teng, Y.; Zhang, J. Design and evaluation of an economic taste-masked dispersible tablet of pyridostigmine bromide, a highly soluble drug with an extremely bitter taste. *Chem. Pharm. Bull.* **2012**, *60*, 1514−1521.

(9) Martin, A.; Tabary, N.; Leclercq, L.; Junthip, J.; Degoutin, S.; Aubert-Viard, F.; Cazaux, F.; Lyskawa, J.; Janus, L.; Bria, M.; Martel, B. Multilayered textile coating based on a β-cyclodextrin polyelectrolyte for the controlled release of drugs. *Carbohydr. Polym.* **2013**, *93*, 718−730.

(10) Nikolic, I. L.; Savic, I. M.; Popsavin, M. M.; Rakic, S. J.; Mihajilov-Krstev, T. M.; Ristic, I. S.; Eric, S. P.; Savić-Gajic, I. M. Preparation, characterization and antimicrobial activity of inclusion complex of biochanin A with (2-hydroxypropyl)-β-cyclodextrin. *J. Pharm. Pharmacol.* **2018**, *70*, 1485−1493.

(11) Wang, X.; Parvathaneni, V.; Shukla, S. K.; Kanabar, D. D.; Muth, A.; Gupta, V. Cyclodextrin Complexation for Enhanced Stability and Non-invasive Pulmonary Delivery of Resveratrol—Applications in Non-small Cell Lung Cancer Treatmen. *AAPS PharmSciTech* **2020**, *21*, No. 183.

(12) Shen, C.; Yang, X.; Wang, Y.; Zhou, J.; Chen, C. Complexation of capsaicin with β-cyclodextrins to improve pesticide formulations: effect on aqueous solubility, dissolution rate, stability, and soil adsorption. *J. Incl. Phenom. Macrocycl. Chem.* **2012**, *72*, 263−274.

(13) Savic, I. M.; Jocic, E.; Nikolic, V. D.; Popsavin, M. M.; Rakic, S. J.; Savic-Gajic, I. M. The effect of complexation with cyclodextrins on the antioxidant and antimicrobial activity of ellagic acid. *Pharm. Dev. Technol.* **2019**, *24*, 410−418.

(14) Inoue, Y.; Suzuki, K.; Ezawa, T.; Murata, I.; Yokota, M.; Tokudome, Y.; Kanamoto, I. Examination of the physicochemical properties of caffeic acid complexed with γ-cyclodextrin. *J. Incl. Phenom. Macrocycl. Chem.* **2015**, *83*, 289−298.

(15) Ezawa, T.; Inoue, Y.; Murata, I.; Suzuki, M.; Takao, K.; Sugita, Y.; Kanamoto, I. Syntheses and crystal structures of two piperine derivatives. *Acta Crystallogr., Sect. E: Crystallogr. Commun.* **2020**, *76*, 646−650.

(16) Ezawa, T.; Inoue, Y.; Murata, I.; Takao, K.; Sugita, Y.; Kanamoto, I. Evaluation of the molecular state of piperine in cyclodextrin complexes by near-infrared spectroscopy and solid-state fluorescence measurements. *Int. J. Med. Chem.* **2019**, *2019*, No. 7530480.

(17) Ezawa, T.; Inoue, Y.; Murata, I.; Takao, K.; Sugita, Y.; Kanamoto, I. Characterization of the dissolution behavior of piperine/cyclodextrins inclusion complexes. *AAPS PharmSciTech* **2018**, *19*, 923−933.

(18) Mangolim, C. S.; Moriwaki, C.; Nogueira, A. C.; Sato, F.; Baesso, M. L.; Neto, A. M.; Matioli, G. Curcumin-β-cyclodextrin inclusion complex: stability, solubility, characterisation by FT-IR, FT-Raman, X-ray diffraction and photoacoustic spectroscopy, and food application. *Food Chem.* **2014**, *153*, 361−370.

(19) Shiozawa, R.; Inoue, Y.; Murata, I.; Kanamoto, I. Effect of antioxidant activity of caffeic acid with cyclodextrins using ground mixture method. *Asian J. Pharm. Sci.* **2018**, *13*, 24−33.

(20) Topchieva, I. N.; Tonelli, A. E.; Panova, I. G.; Matuchina, E. V.; Kalashnikov, F. A.; Gerasimov, V. I.; Rusa, C. C.; Rusa, M.; Hunt, M. A. Two-phase channel structures based on alpha-cyclodextrin-polyethylene glycol inclusion complexes. *Langmuir* **2004**, *20*, 9036−9043.

(21) Guo, X. Q.; Song, L. X.; Dang, Z.; Du, F. Y. A comparative study on the formation and spectral properties of the polypseudorotaxanes of β-cyclodextrin and poly (propylene glycol) under different conditions. *Bull. Chem. Soc. Jpn.* **2009**, *82*, 1209−1213.

(22) Li, N.; Liu, J.; Zhao, X.; Gao, Y.; Zheng, L.; Zhang, J.; Yu, L. Complex formation of ionic liquid surfactant and β-cyclodextrin. *Colloids Surf., A* **2007**, *292*, 196−201.

(23) Giordano, F.; Novak, C.; Moyano, J. R. Thermal analysis of cyclodextrins and their inclusion compounds. *Thermochim. Acta* **2001**, *380*, 123−151.

(24) Christy, A. A. Insights into the chemistry of adsorption of water molecules by cyclodextrins as studied by near infrared spectroscopy. *Adv. Nat. Appl. Sci.* **2015**, *9*, 7−13.

(25) Furune, T.; Ikuta, N.; Ishida, Y.; Okamoto, H.; Nakata, D.; Terao, K.; Sakamoto, N. A study on the inhibitory mechanism for cholesterol absorption by α-cyclodextrin administration. *Beilstein J. Org. Chem.* **2014**, *10*, 2827−2835.

(26) Porter, C. J.; Trevaskis, N. L.; Charman, W. N. Lipids and lipid-based formulations: optimizing the oral delivery of lipophilic drugs. *Nat. Rev. Drug Discovery* **2007**, *6*, 231−248.

(27) Uekaji, Y.; Jo, A.; Ohnishi, M.; Nakata, D.; Terao, K. A new generation of nutra-ceuticals and Cosmeceuticals complexing lipophilic bioactives with γ-cyclodextrin. *Procedia Eng.* **2012**, *36*, 540−550.

(28) Vajda, Š.; Jimenez, R.; Rosenthal, S. J.; Fidler, V.; Fleming, G. R.; Castner, E. W. Femtosecond to nanosecond solvation dynamics in pure water and inside the gamma-cyclodextrin cavity. *J. Chem. Soc., Faraday Trans.* **1995**, *91*, 867−873.

(29) Massin, J.; Dayoub, W.; Mulatier, J.-C.; Aronica, C.; Bretonnière, Y.; Andraud, C. Near-infrared solid-state emitters based on isophorone: synthesis, crystal structure and spectroscopic properties. *Chem. Mater.* **2011**, *23*, 862−873.

(30) Thomas, S. W.; Joly, G. D.; Swager, T. M. Chemical sensors based on amplifying fluorescent conjugated polymers. *Chem. Rev.* **2007**, *107*, 1339−1386.

(31) Debnath, S.; Mishra, J. Understanding the intrinsic fluorescence of piperine in microheterogeneous media: partitioning and loading studies. *New J. Chem.* **2020**, *44*, 8317−8324.

(32) Haque, M. T.; Shams, M. R.; Tahsin, F.; Al Haque, M. M.; Hasan, M. Z.; Al Mahabub, A.; et al. Antidiarrheal activity of methanol extract of Piper sylvaticum (roxb.) stem in mice and in silico molecular docking of its isolated compounds. *Discovery Phytomed.* **2019**, *6*, 92−98.

(33) di Bosco, A. M.; Grieco, P.; Diurno, M. V.; Campiglia, P.; Novellino, E.; Mazzoni, O. Binding Site of Loperamide: Automated Docking of Loperamide in Human l-and d-Opioid Receptors. *Chem. Biol. Drug Des.* **2008**, *71*, 328−335.

https://dx.doi.org/10.1021/acsomega.0c06198
ACS Omega 2021, 6, 6953−6964